

# Constraining Chaplygin models using diffuse supernova neutrino background

Nan Yang<sup>a</sup>, Junji Jia<sup>b</sup>, Xionghui Liu<sup>c,b</sup>, Hongbao Zhang<sup>d,e</sup>

<sup>a</sup>*Glyn O. Phillips Hydrocolloid Research Centre, Hubei University of Technology, Wuhan 430068, China*

<sup>b</sup>*Center for Astrophysics & Center for Theoretical Physics, School of Physics and Technology, Wuhan University, Wuhan, 430072, China*

<sup>c</sup>*Quantum Information Research Center, Shangrao Normal University, Shangrao, Jiangxi 334001, China*

<sup>d</sup>*Department of Physics, Beijing Normal University, Beijing 100875, China*

<sup>e</sup>*Theoretische Natuurkunde, Vrije Universiteit Brussel and The International Solvay Institutes, Pleinlaan 2, B-1050 Brussels, Belgium*

---

## Abstract

In this work, we examine the possibility of using the diffuse supernova neutrino background (DSNB) to test the Chaplygin gas (CG) models of the Universe. With a typical star formation rate  $\psi(z)$ , supernova rate  $R_{\text{SN}}(z)$  and single supernova neutrino spectrum  $dN(E_\nu)/dE_\nu$ , the DSNB flux spectrum  $n(E_\nu)$  in three categories of CG models, the generalized CG (GCG), modified CG (MCG) and extended CG (ECG) models, are studied. It is found that generally the flux spectra take a form similar to a Fermi-Dirac distribution with a peak centered around 4.55-4.78 MeV. The spectrum shape and peak position are primarily determined by  $\psi(z)$ ,  $R_{\text{SN}}(z)$  and  $dN(E_\nu)/dE_\nu$  and only slightly affected by the CG models. However, the height of the spectra in each category of the CG models can vary dramatically for different models in each category, with variances 13.2%, 23.6% and 14.9% for GCG, MCG and ECG categories respectively. The averaged total flux in each category are also different, with the ECG model average 10% and 12% higher than that of the GCG and MCG models. These suggest that the DSNB flux spectrum height and total flux can be used to constrain the CG model parameters, and if the measured to a sub-10% accuracy, might be used to rule out some models.

**Keywords:** Chaplygin gas, diffuse supernova neutrino background, cosmological models

---

## 1. Introduction

The cosmological observation data, including type Ia supernova (SN Ia) [1, 2, 3, 4, 5], cosmic microwave background (CMB) [6, 7, 8, 9], baryon acoustic oscillations (BAO) [10, 11, 12, 13, 14, 15], the observational Hubble data (OHD) [16], implies the late-time cosmic acceleration. The most popular explanation is that about 70% of the energy density of the Universe today are dark energy. One of the simplest form of this energy is the cosmological constant  $\Lambda$  which is used in the  $\Lambda$ -cold dark matter model ( $\Lambda$ CDM) of the Universe. This constant is characterized by the equation of state (EoS) index  $w = -1$ , which is very consistent with the data constrained value  $w = -1.03 \pm 0.03$  [17].

However, the theoretical origin of  $\Lambda$  has not been understood yet. If it was the vacuum energy associated with particle physics then it is hard to explain the

huge gap between the theoretical and observed values [18, 19]. Thus alternative theories attempting to explain the late-time acceleration without using constant dark matter are intensively studied. Broadly, these alternatives can be classified into two categories. The first category is usually inside the framework of general relativity and based on a particular form of matter/field, such as quintessence [20, 21], k-essence [22, 23, 24] and Chaplygin gas (CG) [25, 26, 27, 28, 29, 30, 31, 32, 33, 34, 35, 36, 37, 38, 39, 40] or other fields/interactions. The second category however modifies either the general relativity or the homogenous and isotropic assumption of the universe, such as  $f(R)$  theory [41],  $f(T)$  theory [42, 43], and inhomogeneous models [44, 45].

Among the first category, the CG models recently have gained much attention. It started from the basic CG model with simple EoS [26]

$$P = -\frac{A}{\rho} \quad (1)$$

where  $A$  is a positive constant and then evolved to the

---

*Email addresses:* nanyang27@gmail.com (Nan Yang), junji.jia@whu.edu.cn (Junji Jia), liuxionghui@whu.edu.cn (Xionghui Liu), hzhang@vub.ac.be (Hongbao Zhang)

generalized CG (GCG) model with EoS [25]

$$P = -\frac{A}{\rho^\alpha} \quad (2)$$

where  $0 < \alpha \leq 1$  in order for the Universe to enter the stage dominated by the cosmological constant. Currently, the simple CG model described by Eq. (1) has been ruled out completely [46, 47]. Later on, the EoS was further updated to the so-called modified CG (MCG) form

$$P = B\rho - \frac{A}{\rho^\alpha}, \quad (3)$$

which is essentially a combination of an ordinary fluid obeying a linear barotropic EoS with the GCG fluid. It is also possible to include fluid with constant, quadratic or even higher power barotropic EoS [34, 35, 40] so that the model becomes the extended CG (ECG) with EoS

$$P = \sum_i B_i \rho^i - \frac{A}{\rho^\alpha}, \quad (4)$$

where  $B_i$  are also constants. Clearly, setting proper constants to zero in Eq. (4) will reduce it to (3), which further reduces to (2) when  $B = 0$  and then to (1) when  $\alpha$  is fixed to 1.

These various CG models, together with the  $\Lambda$ CDM have been compared against various observational data, including SN Ia, CMB, BAO, OHD and other data. It is generally found that all these models have some survival region in their respective parameter space.

In this work, we discuss the possibility that these models can be further constrained by the diffuse supernova neutrino background (DSNB). When a star ends its life in the form of a supernova, almost its entire mass is released in the form of an enormous amount of neutrinos whose average energy is at the order  $O(10)$  Mev level. Neutrinos from all supernovae in the history diffuse freely in the Universe and form the DSNB. The evolution of DSNB is influenced by how the Universe expands, just like the CMB or the cosmic neutrino background [48], but at a much higher energy level. With the fast development of the neutrino observatory technologies and increase of observatory size in recent years, the observation of DSNB could be in the reach of a few upcoming neutrino experiment, such as JUNO [49].

In what follows, we first briefly discuss in section 2 the DSNB flux spectrum and the related core collapse (CC) supernova rate and supernova neutrino spectrum. In section 3 we summarize in details the aforementioned models and their corresponding cosmologies which are characterized by the Hubble parameters. We then use

these inputs to compute the expected DSNB flux spectrum for each model in section 4. It will be seen that for the parameters that are allowed by other data, the corresponding DSNB flux spectrum can differ by a large amount. Therefore if observed, the DSNB should provide a new way to severely constraint these models or even rule out some of them.

## 2. The DSNB flux density

The spectrum of DSNB flux in the energy interval  $[E_\nu, E_\nu + dE_\nu]$  emitted in the redshift interval  $[z, z + dz]$  can be calculated using the ‘‘line-of-sight’’ integral method to be [50]

$$dn_\nu(E_\nu) = [R_{\text{SN}}(z)(1+z)^3] \left[ -\frac{dt}{dz} dz \right] \left[ \frac{dN_\nu(E'_\nu)}{dE'_\nu} dE'_\nu \right] (1+z)^{-3}, \quad (5)$$

where  $E'_\nu = (1+z)E_\nu$  is the neutrino energy at redshift  $z$  which is now measured as  $E_\nu$ .  $\frac{dN_\nu(E'_\nu)}{dE'_\nu}$  is the effective neutrino number spectrum for one supernova.  $R_{\text{SN}}(z)$  is the CC supernova rate at redshift  $z$ . The factors  $(1+z)^{\pm 3}$  takes into account the effect of Universe expansion to the volume integral element. The term  $-\frac{dt}{dz}$  is related to the Hubble parameter by

$$-\frac{dt}{dz} = \frac{1}{1+z} \frac{1}{H(z)}. \quad (6)$$

The DSNB flux spectrum is obtained then by integrating Eq. (5) with respect to the redshift

$$n(E_\nu) = \int_0^\infty \left[ R_{\text{SN}}(z) \frac{dN_\nu(E'_\nu)}{dE'_\nu} \right] \left[ \frac{1}{H(z)} \right] dz. \quad (7)$$

Therefore clearly the DSNB flux (7) depend on the cosmological model  $H(z)$  very critically. Besides this, the CC supernova rate  $R_{\text{SN}}(z)$  and supernova spectrum  $\frac{dN_\nu(E'_\nu)}{dE'_\nu}$  are the other two components under the integral. In principle, both of them should depend not only on the redshift but also on other parameters such as the supernova progenitor mass. The  $R_{\text{SN}}(z)$  and  $\frac{dN_\nu(E'_\nu)}{dE'_\nu}$  we used here are in this sense averaged over other factors. Practically, only these averaged quantities are readily available from literature. For the CC supernova rate, it was thought that there were a problem of mismatch between it and the star formation rate [51]. However recently a few promising solution have been proposed including enhancing the initial mass function [52], revised star formation history [53] and change of the stellar mass ranges that end up as CC SNe [54]. After these

solutions, it appears that the current measured CC supernova rate roughly reflect the true rate happens in the Universe. Moreover, since our concentration here is on the effect of cosmological models on the DSNB but not that of the supernova or star formation rates, we will direct adopt the CC supernova rate in Refs. [55, 56], which is

$$R_{\text{SN}}(z) = k \cdot h^2 \cdot \psi(z) \quad (8)$$

where  $k \simeq 0.0091M_{\odot}$  is the number of stars per unit mass that explode as CC SNe,  $h$  is defined as in  $H_0 = 100h \text{ km s}^{-1}\text{Mpc}^{-1}$  and  $\psi(z)$  is the star formation rate given by Ref. [53, 56]

$$\psi(z) = \frac{A(1+z)^C}{1 + ((1+z)/B)^D} [\text{M}_{\odot}\text{year}^{-1}\text{Mpc}^{-3}] \quad (9)$$

with  $A = 0.015$ ,  $B = 2.9$ ,  $C = 2.7$  and  $D = 5.6$ .

For the single supernova neutrino spectrum, we only consider the anti-electron neutrino spectrum because the main detection channel in the observatories such as JUNO is the inverse beta decay process  $\bar{\nu}_e + P \rightarrow e^+ + n$ . This spectrum can be approximated by the pinched Fermi-Dirac spectrum [57, 58]

$$\frac{dN_{\nu}(E'_{\nu})}{dE'_{\nu}} = E_{\bar{\nu}_e, \text{tot}} \frac{120 E'_{\nu}{}^2}{7\pi^4 T^4} \frac{1}{e^{E'_{\nu}/T} + 1}, \quad (10)$$

where we choose  $E_{\bar{\nu}_e, \text{tot}} \sim 5 \times 10^{52}$  erg to represent the typical energy radiated away by the neutrinos during supernova,  $T = 6 \text{ Mev}$  is the radiation temperature.

### 3. The (x)CG models

For the MCG model with EoS (3), solving the energy conservation equation one obtains the energy density of MCG given by

$$\begin{aligned} \rho_{\text{MCG}} &= \rho_{0, \text{MCG}} \left[ A_S + \frac{1 - A_S}{a^{3(1+\alpha)(1+B)}} \right]^{\frac{1}{1+\alpha}} \\ &\equiv \rho_{0, \text{MCG}} f(A_S, B, \alpha, a), \end{aligned} \quad (11)$$

where  $a$  is the scale factor in the Friedmann-Robertson-Walker metric,  $A_S = A/[(B+1)\rho_{0, \text{MCG}}^{\alpha+1}]$  and  $\rho_{0, \text{MCG}}$  is a positive integration constant representing the MCG density today. Further assuming that the Universe is filled with the MCG, regular baryonic matter and regular radiation components  $\rho_{\text{MCG}}$ ,  $\rho_b$ ,  $\rho_r$ , and taking into account the curvature effective energy density  $\rho_{\kappa}$  then the total density  $\rho_t$  becomes

$$\rho_t = \rho_{\text{MCG}} + \rho_b + \rho_r + \rho_{\kappa}. \quad (12)$$

Making use of the Friedman equation, the Hubble parameter is obtained as

$$\begin{aligned} H_{\text{MCG}} &= H_0 \left\{ (1 - \Omega_{0,b} - \Omega_{0,r} - \Omega_{0,\kappa}) f(A_S, B, \alpha, (1+z)^{-1}) \right. \\ &\quad \left. + \Omega_{0,b}(1+z)^3 + \Omega_{0,r}(1+z)^4 + \Omega_{0,\kappa}(1+z)^2 \right\}^{1/2}, \end{aligned} \quad (13)$$

where we have used  $(1+z)^{-1}$  to replace  $a$  and  $\Omega_{0,i}$  ( $i = b, r, \kappa$ ) are today's values of dimensionless energy densities of baryon, radiation and effective curvature respectively. Most of the previous studies on the CG models (see Tables 1 and 3) assumed that  $\Omega_{0,r} = \Omega_{\kappa} = 0$  to simplify the cosmological models. For the DSNB flux calculation given by Eq. (7), there is one more reason that they can be ignored: the neutrino spectrum (10) suppresses exponentially the contribution to the flux from small  $a$  eras, while for the large  $a$  stage it is known that the radiation density as well as the effective curvature parameter are both small (Planck 2018 data yields a value of  $\Omega_{0,\kappa} = 0.001 \pm 0.002$  [17]). Setting  $B = 0$  in Eq. (13) will produce the Hubble parameter for the GCG model

$$\begin{aligned} H_{\text{GCG}} &= H_0 \left\{ (1 - \Omega_{0,b} - \Omega_{0,r} - \Omega_{0,\kappa}) \right. \\ &\quad \left. \times \left[ A_S + (1 - A_S)(1+z)^{3(1+\alpha)} \right]^{\frac{1}{1+\alpha}} \right. \\ &\quad \left. + \Omega_{0,b}(1+z)^3 + \Omega_{0,r}(1+z)^4 + \Omega_{0,\kappa}(1+z)^2 \right\}^{1/2}. \end{aligned} \quad (14)$$

While for the ECG models with EoS (4), the energy conservation equation in the general case are not analytically solvable to obtain solutions like Eq. (11). Only a handful of work are carried out with particularly chosen nonzero  $B_i$  or  $A$  in the EoS (4) [59, 38, 40]. Here we will only concentrate on the following three cases considered by Ref. [40] due to its explicit Hubble parameter formulas that can be directly used by our calculations. First when the sum in Eq. (4) has only two nonzero term  $i = 1$  and  $i = n$ , then denoting  $B_1 = -A$ ,  $B_n = B$ , the EoS becomes

$$P = -A\rho + B\rho^n, \quad (15)$$

and the corresponding Hubble parameter is solved to be

$$\begin{aligned} H_{\text{ECG1}}(z) &= H_0 \left\{ (1 - \Omega_{0,b} - \Omega_{0,r} - \Omega_{0,\kappa}) \right. \\ &\quad \left. \times \left[ A_S + (1 - A_S)(1+z)^{3(A-1)(n-1)} \right]^{\frac{1}{1-n}} \right. \\ &\quad \left. + \Omega_{0,b}(1+z)^3 + \Omega_{0,r}(1+z)^4 + \Omega_{0,\kappa}(1+z)^2 \right\}^{1/2}, \end{aligned} \quad (16)$$

in which  $A_S$ ,  $A$  are parameters converted from  $A$ ,  $B$  and

*n.* When the EoS is given by

$$P = B(\rho + \rho^2) - \frac{A}{\rho^{1/2}}, \quad (17)$$

the Hubble parameter will be

$$H_{\text{ECG2}}(z) = H_0 \left[ 1 + \frac{1}{X^2} (1+z)^{[9(B+1)+15X^2B]/2} \right], \quad (18)$$

where  $X$  is some effective parameter related to  $B$  in Eq. (17). Finally when the EoS is

$$P = B(\rho + \rho^2 + \rho^3) - \frac{A}{\rho^{1/2}}, \quad (19)$$

the Hubble parameter is

$$H_{\text{ECG3}}(z) = H_0 \left[ 1 + \frac{1}{Y^2} (1+z)^{[9(B+1)+15Y^2B+21Y^4B]/2} \right]. \quad (20)$$

Again,  $Y$  here is an effective parameter related to  $B$  in Eq. (19).

The  $\Lambda$ CDM model we used to compare to the above models is given by

$$H_{\Lambda\text{CDM}} = H_0 \left[ \Omega_m (1+z)^3 + \Omega_\Lambda \right]^{1/2}, \quad (21)$$

where we take  $\Omega_\Lambda = 0.685$ ,  $\Omega_m = 0.315$  and  $H_0 = 67.4 \text{ km s}^{-1} \text{ Mpc}^{-1}$  [17].

As mentioned early, these models were constrained using different combination of data sets and methods. Consequently, the obtained values of parameters are also slightly different even for the same kind of CG models. Here we summarize the values of the parameters in the GCG models (Table 1), MCG models (Table 2) and ECG models (Table 3) according to the data sets that were used.

#### 4. The DSNB flux in (x)CG cosmologies

With the CC supernova rate (8), star formation rate (9), supernova neutrino spectrum (10) as well as the cosmological models described by Eqs. (13), (14), (16), (18), (20) and (21), we can now integrate Eq. (7) to find the DSNB flux for all models with parameters listed in Tables 1, 2 and 3. The results are shown separately for the GCG, MCG and ECG models in Fig. 1 (a), (b) and (c).

It is seen that for all models with different values of parameters, the spectrum takes the shape similar to a Fermi-Dirac distribution, with a single peak centered around 4.55-4.78 MeV (the exact peak position of each

model is given in Tables 1-3). This suggest that the shape of the spectrum, as well as the location of the peak, is not primarily determined by the cosmological model but other factors in the integral (7), namely the SN spectrum, star formation and supernova rate. The cosmological models when limited by the range of the parameters in Tables 1-3 however, still can weakly affect the peak positions. This point is reflected by the fact that for the ECG models, especially the models ECG2 and ECG3 in Fig. 1 (c), their peak positions are shifted to a slightly lower value comparing to those of the GCG and MCG models. A simple statistic analysis shows that the peak position average for the GCG models is  $4.72 \pm 0.04$  MeV. Average peak position of the MCG models is found to be the same as the GCG models, but that of the ECG models is  $4.63 \pm 0.11$  MeV. Therefore the mean peak position of the ECG models considered here is about 2.0% lower than that of the GCG or ECG models.

On the contrary, the height of the peaks, unlike the spectrum shape or the peak position, is strongly affected by the cosmological models (see Tables 1-3 for the exact peak height for each model). From Fig. 1 (a), it is seen that the maxima of the DSNB flux spectra in different GCG models can vary from  $0.487 \text{ MeV}^{-1} \text{ cm}^{-2} \text{ s}^{-1}$  to  $0.551 \text{ MeV}^{-1} \text{ cm}^{-2} \text{ s}^{-1}$ , a difference about 13.2%. For the MCG models, Fig. 1 (b) shows that the highest and lowest of the peaks are respectively  $0.443 \text{ MeV}^{-1} \text{ cm}^{-2} \text{ s}^{-1}$  and  $0.548 \text{ MeV}^{-1} \text{ cm}^{-2} \text{ s}^{-1}$  with a difference of 23.6%. The peak height in different ECG models ranges from  $0.548 \text{ MeV}^{-1} \text{ cm}^{-2} \text{ s}^{-1}$  to  $0.630 \text{ MeV}^{-1} \text{ cm}^{-2} \text{ s}^{-1}$ , which corresponds to a difference of 14.9%. It is clear that the DSNB flux spectrum height is very sensitive to the cosmological model, and this suggests that the future measured DSNB flux spectrum will be usable to constraint the Chaplygin gas models. If this data is measured to an accuracy of sub-10% level, then it might even be used to tell which Chaplygin gas is more viable.

We also integrated the flux spectrum over energy to obtain the total flux for each model and then averaged over the same kind of models. It is found that for the GCG models considered in Table 1, MCG models in Table 2 and ECG models in Table 3, the average fluxes are respectively about  $5.66 \text{ cm}^{-2} \text{ s}^{-1}$ ,  $5.56 \text{ cm}^{-2} \text{ s}^{-1}$  and  $6.23 \text{ cm}^{-2} \text{ s}^{-1}$ . The former two are close to that of the  $\Lambda$ CDM model given in Eq. (21) which is  $5.60 \text{ cm}^{-2} \text{ s}^{-1}$  and the ECG model flux is about 10%-12% higher than them. Therefore the total flux can also be used to constraint these models, even if the energy resolved spectrum is not easily obtained in the initial stages of the DSNB measurements.

Table 1: The GCG model parameters in various references. See Ref. [36] for the Growth and  $\sigma_8$  data. The last two columns are the peak positions and heights in Fig. 1(a) with units MeV and  $\text{MeV}^{-1}\text{cm}^{-2}\text{s}^{-1}$  respectively.

Model #	$\alpha$	$A_S$	Data set	Ref.	P. P.	P. H.
GCG1	0.4	0.83	CMB+Quasar+SN	[27]	4.762	0.551
GCG2	0.1	0.77	CMB	[28]	4.727	0.512
GCG3	0.00126	0.775	BAO+CMB+SN	[60]	4.707	0.525
GCG4	0.141	0.819	BAO+CMB+Growth +OHD+SN+ $\sigma_8$	[36]	4.714	0.535
GCG5	0.20	0.77	BAO+CMB+SN	[37]	4.755	0.487
GCG6	-0.100	0.738	BAO+OHD+SN	[38]	4.696	0.532
GCG7	-0.069	0.753	BAO+OHD+SN	[38]	4.702	0.533
GCG8	0.023	0.7720	BAO+CMB+OHD+SN	[39]	4.716	0.528
GCG9	0.4056	0.8846	BAO+CMB+OHD	[40]	4.728	0.548

Table 2: The MCG model parameters in various references. See Ref. [31, 61] for the CBF data and Ref. [33, 36] for the Growth and  $\sigma_8$  data. The last two columns are the peak positions and heights in Fig. 1(b) with units MeV and  $\text{MeV}^{-1}\text{cm}^{-2}\text{s}^{-1}$  respectively.

Model #	$\alpha$	$A_S$	$B$	Data set	Ref.	P. P.	P. H.
MCG1	1.724	0.822	-0.085	BAO+CMB+SN	[29]	4.770	0.443
MCG2	0.11	0.8	0.06	OHD	[30]	4.778	0.487
MCG3	0.1079	0.7788	0.00189	BAO+CBF+CMB +OHD+SN	[31]	4.733	0.515
MCG4	0.000727	0.782	0.000777	BAO+CMB+SN	[32]	4.703	0.524
MCG5	0.002	0.769	0.008	Growth+OHD+ $\sigma_8$	[33]	4.716	0.516
MCG6	0.1905	0.8252	0.0046	BAO+CMB+Growth +OHD+SN+ $\sigma_8$	[36]	4.725	0.529
MCG7	0.538	0.714	-0.166	BAO+OHD+SN	[38]	4.664	0.534
MCG8	0.613	0.716	-0.176	BAO+OHD+SN	[38]	4.662	0.534
MCG9	0.5218	0.9036	0.0067	BAO+CMB+OHD	[40]	4.740	0.548

Table 3: The ECG model parameters in three cases. The last two columns are the peak positions and heights in Fig. 1(c) with units MeV and  $\text{MeV}^{-1}\text{cm}^{-2}\text{s}^{-1}$  respectively.

Model #	Parameters	Data set	Ref.	P. P.	P. H.
ECG1	$A_S = 0.9028, A = 0.0066, n = -0.5146$	BAO+CMB+OHD	[40]	4.740	0.548
ECG2	$B = -0.037662, X = 2.83633$	BAO+CMB+OHD	[40]	4.554	0.630
ECG3	$B = -0.00328, Y = 2.83641$	BAO+CMB+OHD	[40]	4.554	0.630

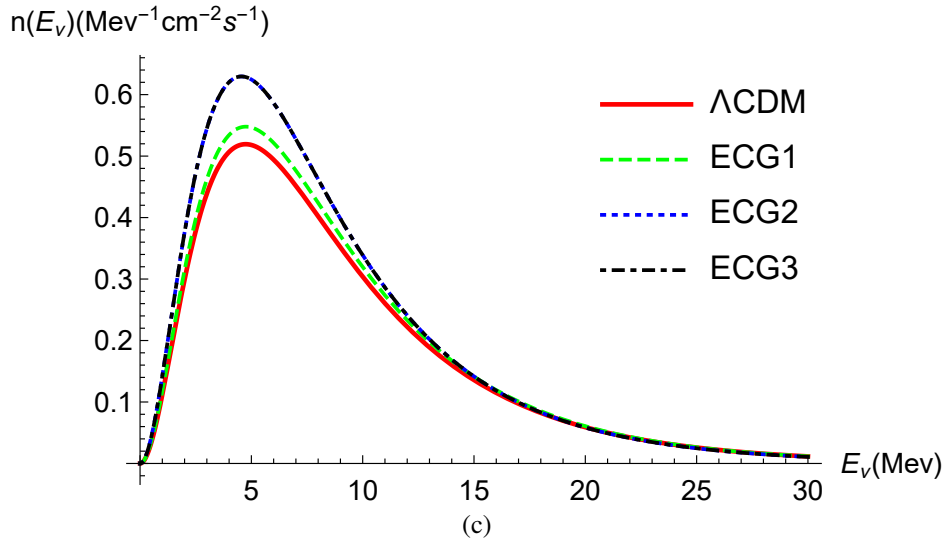
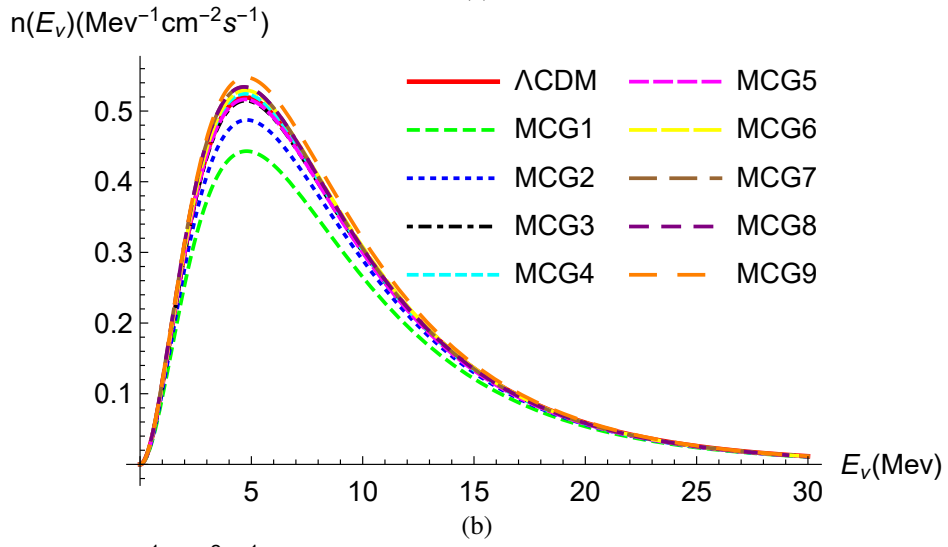
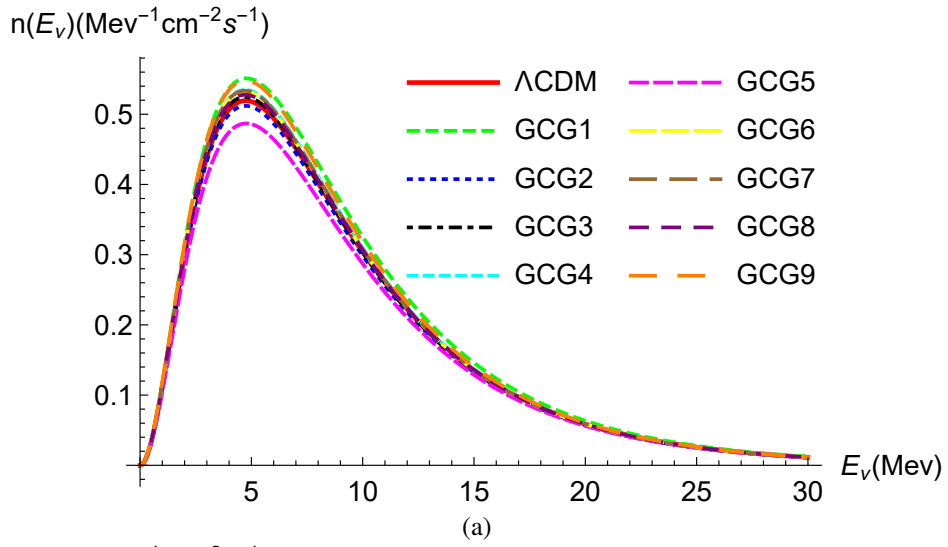


Figure 1: The flux spectra in GCG models (a), MCG models (b) and ECG models (c). The flux spectrum in  $\Lambda$ CDM model is drawn in each subplot using red solid line. See last two columns in each of the Tables 1-3 for the exact peak positions and heights.

## 5. Conclusion and Discussions

Using a standard supernova neutrino spectrum and typical CC supernova and star formation rates, we obtained the DSNB flux spectra in various GCG, MCG and ECG models. It is found that generally the shape and peak position of the flux spectrum is largely determined by the supernova neutrino spectrum, supernova and star formation rates. Different CG models can only cause a difference of 2.0% in the peak positions. The spectrum height however depends strongly on the Chaplygin gas model used to do the calculation. The variance in peak heights among different GCG models, MCG models and ECG models can reach respectively 13.2%, 23.6% and 14.9%. This suggests a great potential for the DSNB to constraint these models. The averaged total flux for ECG models is 10%-12% higher than the GCG and MCG models and therefore the total DSNB flux can also be used to discriminate the Chaplygin models.

Regarding the possible extensions of the work, the following comments are in order. Although in this work we used the Chaplygin gas models for the cosmology, it is clear from the flux spectrum formula (7) that for other cosmological models, such as quintessence, k-essence theories, or even modified gravity cosmologies, it is straight forward to compute a similar DSNB flux spectrum and use it to constrain the corresponding cosmological model. We are currently working along this direction.

## Acknowledgement

This work is supported by the National Nature Science Foundation of China No. 11504276, 11675015, and No. 31571797. In addition, HZ is supported in part by FWO-Vlaanderen through the project G006918N, and by the Vrije Universiteit Brussel through the Strategic Research Program “High-Energy Physics”. He is also an individual FWO Fellow supported by 12G3515N.

## References

- [1] A. G. Riess *et al.* [Supernova Search Team], *Astron. J.* **116**, 1009 (1998) doi:10.1086/300499 [astro-ph/9805201].
- [2] S. Perlmutter *et al.* [Supernova Cosmology Project Collaboration], *Astrophys. J.* **517**, 565 (1999) doi:10.1086/307221 [astro-ph/9812133].
- [3] M. Kowalski *et al.* [Supernova Cosmology Project Collaboration], *Astrophys. J.* **686**, 749 (2008) doi:10.1086/589937 [arXiv:0804.4142 [astro-ph]].
- [4] R. Amanullah *et al.*, *Astrophys. J.* **716**, 712 (2010) doi:10.1088/0004-637X/716/1/712 [arXiv:1004.1711 [astro-ph.CO]].
- [5] N. Suzuki *et al.* [Supernova Cosmology Project Collaboration], *Astrophys. J.* **746**, 85 (2012) doi:10.1088/0004-637X/746/1/85 [arXiv:1105.3470 [astro-ph.CO]].
- [6] D. N. Spergel *et al.* [WMAP Collaboration], *Astrophys. J. Suppl.* **148**, 175 (2003) doi:10.1086/377226 [astro-ph/0302209].
- [7] E. Komatsu *et al.* [WMAP Collaboration], *Astrophys. J. Suppl.* **180**, 330 (2009) doi:10.1088/0067-0049/180/2/330 [arXiv:0803.0547 [astro-ph]].
- [8] E. Komatsu *et al.* [WMAP Collaboration], *Astrophys. J. Suppl.* **192**, 18 (2011) doi:10.1088/0067-0049/192/2/18 [arXiv:1001.4538 [astro-ph.CO]].
- [9] <https://lambda.gsfc.nasa.gov/product/map/current/>
- [10] D. J. Eisenstein *et al.* [SDSS Collaboration], *Astrophys. J.* **633**, 560 (2005) doi:10.1086/466512 [astro-ph/0501171].
- [11] K. N. Abazajian *et al.* [SDSS Collaboration], *Astrophys. J. Suppl.* **182**, 543 (2009) doi:10.1088/0067-0049/182/2/543 [arXiv:0812.0649 [astro-ph]].
- [12] W. J. Percival *et al.* [SDSS Collaboration], *Mon. Not. Roy. Astron. Soc.* **401**, 2148 (2010) doi:10.1111/j.1365-2966.2009.15812.x [arXiv:0907.1660 [astro-ph.CO]].
- [13] F. Beutler *et al.*, *Mon. Not. Roy. Astron. Soc.* **416**, 3017 (2011) doi:10.1111/j.1365-2966.2011.19250.x [arXiv:1106.3366 [astro-ph.CO]].
- [14] C. Blake *et al.*, *Mon. Not. Roy. Astron. Soc.* **418**, 1707 (2011) doi:10.1111/j.1365-2966.2011.19592.x [arXiv:1108.2635 [astro-ph.CO]].
- [15] G. Hinshaw *et al.* [WMAP Collaboration], *Astrophys. J. Suppl.* **208**, 19 (2013) doi:10.1088/0067-0049/208/2/19 [arXiv:1212.5226 [astro-ph.CO]].
- [16] J. Simon, L. Verde and R. Jimenez, *Phys. Rev. D* **71**, 123001 (2005) doi:10.1103/PhysRevD.71.123001 [astro-ph/0412269].
- [17] N. Aghanim *et al.* [Planck Collaboration], arXiv:1807.06209 [astro-ph.CO].
- [18] S. Weinberg, *Rev. Mod. Phys.* **61**, 1 (1989) doi:10.1103/RevModPhys.61.1
- [19] S. M. Carroll, *Living Rev. Rel.* **4**, 1 (2001) doi:10.12942/lrr-2001-1 [astro-ph/0004075].
- [20] I. Zlatev, L. M. Wang and P. J. Steinhardt, *Phys. Rev. Lett.* **82**, 896 (1999) doi:10.1103/PhysRevLett.82.896 [astro-ph/9807002].
- [21] L. Amendola, *Phys. Rev. D* **62**, 043511 (2000) doi:10.1103/PhysRevD.62.043511 [astro-ph/9908023].
- [22] C. Armendariz-Picon, V. F. Mukhanov and P. J. Steinhardt, *Phys. Rev. Lett.* **85**, 4438 (2000) doi:10.1103/PhysRevLett.85.4438 [astro-ph/0004134].
- [23] C. Armendariz-Picon, V. F. Mukhanov and P. J. Steinhardt, *Phys. Rev. D* **63**, 103510 (2001) doi:10.1103/PhysRevD.63.103510 [astro-ph/0006373].
- [24] R. J. Scherrer, *Phys. Rev. Lett.* **93**, 011301 (2004) doi:10.1103/PhysRevLett.93.011301 [astro-ph/0402316].
- [25] M. C. Bento, O. Bertolami and A. A. Sen, *Phys. Rev. D* **66**, 043507 (2002) doi:10.1103/PhysRevD.66.043507 [gr-qc/0202064].
- [26] V. Gorini, A. Kamenshchik and U. Moschella, *Phys. Rev. D* **67**, 063509 (2003) doi:10.1103/PhysRevD.67.063509 [astro-ph/0209395].
- [27] M. d. C. Bento, O. Bertolami and A. A. Sen, *Phys. Rev. D* **67**, 063003 (2003) doi:10.1103/PhysRevD.67.063003 [astro-ph/0210468].
- [28] T. Barreiro, O. Bertolami and P. Torres, *Phys. Rev. D* **78**, 043530 (2008) doi:10.1103/PhysRevD.78.043530 [arXiv:0805.0731 [astro-ph]].
- [29] J. Lu, L. Xu, J. Li, B. Chang, Y. Gui and H. Liu, *Phys. Lett. B* **662**, 87 (2008) doi:10.1016/j.physletb.2008.03.005

- [arXiv:1004.3364 [astro-ph.CO]].
- [30] P. Thakur, S. Ghose and B. C. Paul, *Mon. Not. Roy. Astron. Soc.* **397**, 1935 (2009) doi:10.1111/j.1365-2966.2009.15015.x [arXiv:0905.2281 [astro-ph.CO]].
- [31] J. Lu, L. Xu, Y. Wu and M. Liu, *Gen. Rel. Grav.* **43**, 819 (2011) doi:10.1007/s10714-010-1103-4 [arXiv:1105.1870 [astro-ph.CO]].
- [32] L. Xu, Y. Wang and H. Noh, *Eur. Phys. J. C* **72**, 1931 (2012) doi:10.1140/epjc/s10052-012-1931-3 [arXiv:1204.5571 [astro-ph.CO]].
- [33] B. C. Paul and P. Thakur, *JCAP* **1311**, 052 (2013) doi:10.1088/1475-7516/2013/11/052 [arXiv:1306.4808 [astro-ph.CO]].
- [34] E. O. Kahya, M. Khurshudy, B. Pourhassan, R. Myrzakulov and A. Pasqua, *Eur. Phys. J. C* **75**, no. 2, 43 (2015) doi:10.1140/epjc/s10052-015-3263-6 [arXiv:1402.2592 [gr-qc]].
- [35] B. Pourhassan and E. O. Kahya, *Adv. High Energy Phys.* **2014**, 231452 (2014) doi:10.1155/2014/231452 [arXiv:1405.0667 [gr-qc]].
- [36] B. C. Paul, P. Thakur and A. Beesham, *Astrophys. Space Sci.* **361**, no. 10, 336 (2016) doi:10.1007/s10509-016-2916-8 [arXiv:1410.6588 [astro-ph.CO]].
- [37] W. T. Zhu, P. X. Wu and H. W. Yu, *Chin. Phys. Lett.* **32**, no. 5, 059501 (2015). doi:10.1088/0256-307X/32/5/059501
- [38] G. S. Sharov, *JCAP* **1606**, no. 06, 023 (2016) doi:10.1088/1475-7516/2016/06/023 [arXiv:1506.05246 [gr-qc]].
- [39] P. Thakur, *Pramana* **88**, no. 3, 51 (2017). doi:10.1007/s12043-016-1358-8
- [40] B. C. Paul, P. Thakur and A. Saha, *Pramana* **89**, no. 2, 29 (2017). doi:10.1007/s12043-017-1417-9
- [41] T. P. Sotiriou and V. Faraoni, *Rev. Mod. Phys.* **82**, 451 (2010) doi:10.1103/RevModPhys.82.451 [arXiv:0805.1726 [gr-qc]].
- [42] B. Li, T. P. Sotiriou and J. D. Barrow, *Phys. Rev. D* **83**, 064035 (2011) doi:10.1103/PhysRevD.83.064035 [arXiv:1010.1041 [gr-qc]].
- [43] Y. F. Cai, S. Capozziello, M. De Laurentis and E. N. Saridakis, *Rept. Prog. Phys.* **79**, no. 10, 106901 (2016) doi:10.1088/0034-4885/79/10/106901 [arXiv:1511.07586 [gr-qc]].
- [44] V. Marra and A. Notari, *Class. Quant. Grav.* **28**, 164004 (2011) doi:10.1088/0264-9381/28/16/164004 [arXiv:1102.1015 [astro-ph.CO]].
- [45] K. Bolejko, M. N. Celerier and A. Krasinski, *Class. Quant. Grav.* **28**, 164002 (2011) doi:10.1088/0264-9381/28/16/164002 [arXiv:1102.1449 [astro-ph.CO]].
- [46] X. Zhang, F. Q. Wu and J. Zhang, *JCAP* **0601**, 003 (2006) doi:10.1088/1475-7516/2006/01/003 [astro-ph/0411221].
- [47] K. Liao, Y. Pan and Z. H. Zhu, *Res. Astron. Astrophys.* **13**, 159 (2013) doi:10.1088/1674-4527/13/2/003 [arXiv:1210.5021 [astro-ph.CO]].
- [48] J. Jia and H. b. Zhang, *JCAP* **0812**, 002 (2008) doi:10.1088/1475-7516/2008/12/002 [arXiv:0809.2597 [astro-ph]].
- [49] F. An *et al.* [JUNO Collaboration], *J. Phys. G* **43**, no. 3, 030401 (2016) doi:10.1088/0954-3899/43/3/030401 [arXiv:1507.05613 [physics.ins-det]].
- [50] S. Ando and K. Sato, *New J. Phys.* **6**, 170 (2004) doi:10.1088/1367-2630/6/1/170 [astro-ph/0410061].
- [51] S. Horiuchi, J. F. Beacom, C. S. Kochanek, J. L. Prieto, K. Z. Stanek and T. A. Thompson, *Astrophys. J.* **738**, 154 (2011) doi:10.1088/0004-637X/738/2/154 [arXiv:1102.1977 [astro-ph.CO]].
- [52] G. J. Mathews, J. Hidaka, T. Kajino and J. Suzuki, *Astrophys. J.* **790**, 115 (2014) doi:10.1088/0004-637X/790/2/115 [arXiv:1405.0458 [astro-ph.CO]].
- [53] P. Madau and M. Dickinson, *Ann. Rev. Astron. Astrophys.* **52**, 415 (2014) doi:10.1146/annurev-astro-081811-125615 [arXiv:1403.0007 [astro-ph.CO]].
- [54] J. Hidaka, T. Kajino and G. J. Mathews, *Astrophys. J.* **827**, no. 1, 85 (2016). doi:10.3847/0004-637X/827/1/85
- [55] L. G. Strolger *et al.*, *Astrophys. J.* **813**, no. 2, 93 (2015) doi:10.1088/0004-637X/813/2/93 [arXiv:1509.06574 [astro-ph.GA]].
- [56] T. Petrushevska *et al.*, *Astron. Astrophys.* **594**, A54 (2016) doi:10.1051/0004-6361/201628925 [arXiv:1607.01617 [astro-ph.GA]].
- [57] G. G. Raffelt, Chicago, USA: Univ. Pr. (1996) 664 p
- [58] J. F. Beacom, *Ann. Rev. Nucl. Part. Sci.* **60**, 439 (2010) doi:10.1146/annurev.nucl.010909.083331 [arXiv:1004.3311 [astro-ph.HE]].
- [59] E. O. Kahya and B. Pourhassan, *Astrophys. Space Sci.* **353**, no. 2, 677 (2014). doi:10.1007/s10509-014-2069-6
- [60] L. Xu, J. Lu and Y. Wang, *Eur. Phys. J. C* **72**, 1883 (2012) doi:10.1140/epjc/s10052-012-1883-7 [arXiv:1204.4798 [astro-ph.CO]].
- [61] S. W. Allen, D. A. Rapetti, R. W. Schmidt, H. Ebeling, G. Morris and A. C. Fabian, *Mon. Not. Roy. Astron. Soc.* **383**, 879 (2008) doi:10.1111/j.1365-2966.2007.12610.x [arXiv:0706.0033 [astro-ph]].
- [62] T. Regimbau, *Res. Astron. Astrophys.* **11**, 369 (2011) doi:10.1088/1674-4527/11/4/001 [arXiv:1101.2762 [astro-ph.CO]].
- [63] X. J. Zhu, E. Howell, T. Regimbau, D. Blair and Z. H. Zhu, *Astrophys. J.* **739**, 86 (2011) doi:10.1088/0004-637X/739/2/86 [arXiv:1104.3565 [gr-qc]].
- [64] B. P. Abbott *et al.* [LIGO Scientific and Virgo Collaborations], *Phys. Rev. Lett.* **116**, no. 13, 131102 (2016) doi:10.1103/PhysRevLett.116.131102 [arXiv:1602.03847 [gr-qc]].